Anisotropic phonon conduction and lattice distortions in colossal-magnetoresistance bilayer manganite $(La_{1-z}Pr_z)_{1.2}Sr_{1.8}Mn_2O_7$ ($z=0$, 0.2, 0.4, and 0.6) single crystals

M. Matsukawa, M. Narita, T. Nishimura, and M. Yoshizawa
Department of Materials Science and Technology, Iwate University, Morioka 020-8551, Japan

M. Apostu, R. Suryanarayanan, and A. Revcolevschi
Laboratoire de Physico-Chimie de L'etat Solide, CNRS, UMR 8648 Universite Paris-Sud, 91405 Orsay, France

K. Itoh
National Institute for Materials Science, Tsukuba 305-0003, Japan

N. Kobayashi
Institute for Materials Research, Tohoku University, Sendai 980-8577, Japan

(Received 3 June 2002; revised manuscript received 9 December 2002; published 31 March 2003)

We have undertaken a systematic study of thermal conductivity as a function of temperature and magnetic field of single crystals of the compound $(La_{1-z}Pr_z)_{1.2}Sr_{1.8}Mn_2O_7$ for $z(Pr)=0.2$,0.4, and 0.6. The lattice distortion due to Pr substitution and anisotropic thermal conductivity in bilayer manganites are discussed on the basis of different relaxation models of local lattice distortions in metal and insulating states proposed by Medarde *et al.* The giant magnetothermal effect is scaled as a function of magnetization and discussed on the basis of a systematic variation of the occupation of the e_g-electron orbital states due to Pr substitution.

DOI: 10.1103/PhysRevB.67.104433 PACS number(s): 63.90.+t, 72.15.Gd

I. INTRODUCTION

Since the discovery of colossal magnetoresistance (CMR) in the hole-doped perovskite manganites $Ln_{1-x}D_x$ MnO_3 (Ln= trivalent rare earth; D= divalent alkaline earth Ca, Sr, Ba, Pb), extensive studies of the field-induced complex physics exhibited by these CMR compounds have been reported.[1] Though the double-exchange (DE) mechanism[2] plays a major role in explaining some of the properties, a quantitative model to account for the insulator-metal transition and the CMR effect is yet to be proposed. In the DE model, the carriers are strongly ferromagnetically coupled, due to Hund's rule coupling, to the Mn core which also results in the hopping of electrons between the Mn ions. However, it was pointed out that the coupling of carriers to local Jahn-Teller(JT) distortions and to the Mn spins must also be considered.[3] Further, several recent experiments seem to support the phase-separation model.[4] Thermal transport measurements provide additional crucial information on the various scattering mechanisms of thermal carriers such as electrons and phonons and are expected to improve the understanding of some of the phenomena encountered in the manganites. There have been relatively few reports[5–8] on thermal transport in cubic manganites. The thermal conductivity of cubic manganites has been discussed on the basis of static and dynamic lattice distortions by several authors. It should be noted that the $Ln_{1-x}D_x$ MnO_3 cubic perovskite compounds belong to the Ruddlesden-Popper series generally described as $(Ln,D)_{n+1}Mn_nO_{3n+1}$ with $n=\infty$. For $n=2$, one obtains the bilayer Mn perovskite $(Ln,D)_3$ Mn_2O_7, in which two MnO_2 layers are stacked with $(Ln,D)_2O_2$ layers along the c axis of the structure. The reduced dimensionality of these compounds has been shown to have interesting consequences on the physical properties. Let us note that the optimally hole-doped compound $La_{1.2}Sr_{1.2}Mn_2O_7$ ($x=0.4$) exhibits a CMR of more than 98% near the paramagnetic insulator (PI) to ferromagnetic metal (FM) transition temperature $T_c=\sim 120$ K.[9] The thermal conductivity measurements of the double-layer manganite, $La_{1.2}Sr_{1.2}Mn_2O_7$ were reported recently indicating an enhanced giant magnetothermal effect due to its layered structure.[10] For the end member $x=0$ $LaMnO_3$, which is a cubic compound with JT distortions, it was reported that the value of κ measured on a stoichiometric single crystal corresponds to a thermally good conductor, such as an ideal phonon gas.[11] On the other hand, the end member $x=1$ compound $CaMnO_3$, without JT active Mn sites, shows a higher thermal conduction in comparison to the low-κ data obtained for the hole-doped compounds.[8] Therefore, it is desirable to examine the close relationship existing between the lattice distortion and thermal conductivity in layered manganites.

In this paper, we report a systematic study of thermal conductivity as a function of temperature and magnetic field of single crystals of the compound $(La_{1-z}Pr_z)_{1.2}Sr_{1.8}Mn_2O_7$, for $z(Pr)=0.2$,0.4, and 0.6. Keeping the hole doping fixed at $x=0.4$, the chemical pressure effect due to substitution of Pr on La-ion sites enhances anisotropic lattice parameters[12,13] and results in a variation of the e_g-electron character, as reported in (Ref. 14). The lattice distortion due to Pr substitution and the anisotropic thermal conductivity in bilayer manganites were discussed on the basis of different relaxation models of local lattice distortions in metal and insulating states proposed by Medarde *et al.*[15] Next, the giant magnetothermal resistivity was scaled as a function of magnetization and discussed on the basis of a systematic variation in e_g-electron orbital states.

II. EXPERIMENT

Single crystals of $(La_{1-z}Pr_z)_{1.2}Sr_{1.8}Mn_2O_7$ ($z=0$, 0.2, 0.4, and 0.6) were grown from sintered rods of the same nominal composition by the floating-zone method, using a mirror furnace. Crystals could be easily cleaved to yield shiny surfaces. X-ray Laue patterns have indicated the cleaved surface to be along the ab plane of the structure and therefore the c axis perpendicular to it. An x-ray powder pattern taken on a small part of the cleaved crystal did not indicate the presence of any additional phases. The calculated lattice parameters are listed in Refs. 12 and 13. The Pr substitution at La ion sites resulted in a small contraction of the a-axis parameter and an expansion of the c axis parameter. Energy-dispersive x-ray analyses of the cleaved surface revealed the compositions of the two samples to be close to those of the respective sintered rods. The dimensions of the crystals used in the experiments reported here were typically 3.4×2.8 mm^2 in the ab plane and 1.0 mm along the c axis.

The end member compound $Sr_3Mn_2O_7$ was prepared by a powder sintering technique under the annealing condition 1650°C for 12 h first reported by Mizutani *et al.*[16] and by Mitchell *et al.*[17] After rapidly cooling it down to room temperatures to prevent decomposition, the polycrystalline sample was postannealed at 400°C for 24 h to remove its oxygen deficiency. The dimensions of the cylindrical sintered sample used in the thermal measurement were 4.4 mm in diameter and 8 mm along the longitudinal direction. The x-ray powder pattern of this sample showed that the sample obtained consists mainly of a single phase with the 327 crystal structure. The magnetization measurements also revealed that the present sample shows an antiferromagnetic transition around $T_N \simeq 160$ K.[17] The thermal conductivity, both in the ab plane and along the c axis of the crystal, was measured by means of the steady-state heat-flow method using a Gifford-McMahon type cryocooler in zero field. Magnetothermal conductivity measurements were carried out at the National Research Institute for Metals and at the High Field Laboratory for Superconducting Materials, Institute for Materials Research, Tohoku University. The resistivity in the ab plane of the crystal was measured using a conventional four-probe technique. The zero-field-cooled magnetization measurements were made by superconducting quantum interference device using a magnetometer both at Iwate University and in Orsay.

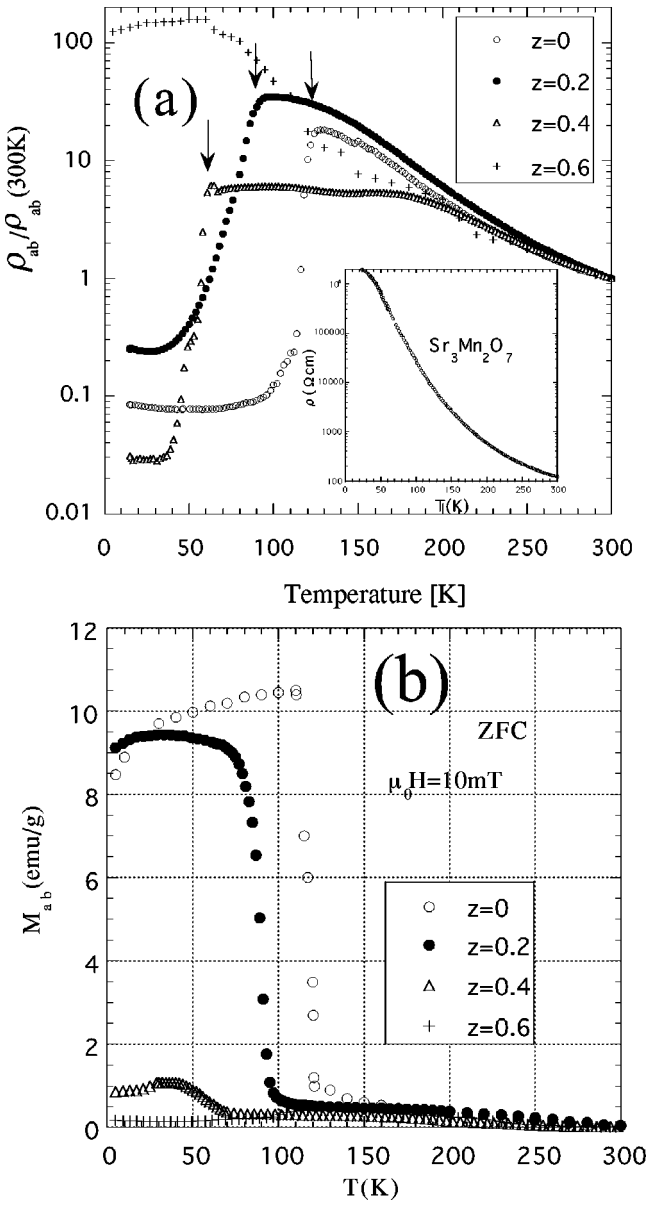

FIG. 1. (a) ab-plane normalized resistivity ρ_{ab} and (b) ab-plane magnetization M_{ab} for $(La_{1-z}Pr_z)_{1.2}Sr_{1.8}Mn_2O_7$ ($z=0$, 0.2, 0.4, and 0.6) single crystals. The arrows denote the PI to FM transition temperature. The ρ data of the polycrystalline sample $Sr_3Mn_2O_7$ are also shown in the inset of (a).

III. RESULTS AND DISCUSSION

Figures 1(a) and 1(b) present the ab plane normalized resistivity ρ_{ab} and the ab plane magnetization M_{ab} of our samples ($z=0$, 0.2, 0.4, and 0.6) as a function of temperature. The ρ data of the polycrystalline sample $Sr_3Mn_2O_7$ are also shown in the inset of Fig. 1 (a). For the $z=0$ crystal, the value of ρ_{ab} dropped sharply at $\sim$120 K, close to the insulating to metallic transition ,with decreasing temperature. This temperature was reduced to $\sim$60 K in the sample with $z=0.4$. Finally, the $z=0.6$ sample showed neither an insulator to metal transition nor a paramagnetic to ferromagnetic transition. The temperature variation of the resistivity of the $x=1$ sample showed a negative curvature over the whole measured range and the value of ρ rapidly increased by more than four orders of magnitude, up to 2×10^6 Ω cm at 20 K from $\sim$100Ω cm at room temperature (RT), which is in sharp contrast with the typical value of $\sim$0.1Ω cm at RT for Pr-substituted samples.[12,13] Recently, a theoretical band calculation[18] predicted that the bilayer perovskite $Sr_3Mn_2O_7$ is an antiferromagnetic insulator with an indirect gap of 0.45 eV, which is qualitatively in good agreement with our magnetization and resistivity data. Moreover, the electronic structure of this compound is expected to be similar to that of the cubic perovskite end member $CaMnO_3$.

The ab-plane and the c-axis thermal conductivity of $(La_{1-z}Pr_z)_{1.2}Sr_{1.8}Mn_2O_7$ ($z=0$, 0.2 ,0.4, and 0.6) single

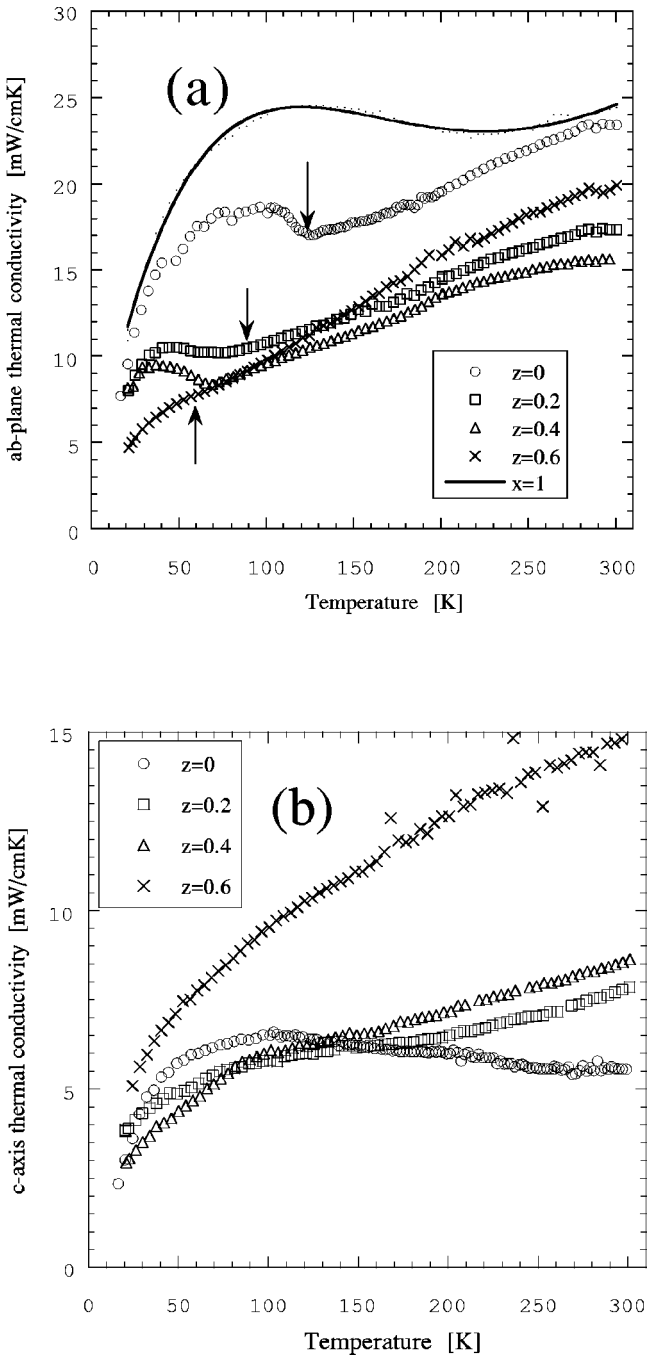

FIG. 2. (a) ab-plane and (b) c-axis thermal conductivity of $(La_{1-z}Pr_z)_{1.2}Sr_{1.8}Mn_2O_7$ ($z=0$, 0.2, 0.4, and 0.6) single crystals. The arrows denote the PI to FM transition temperature. For comparison, the temperature variation of polycrystalline $Sr_3Mn_2O_7$ ($x=1$) is also presented in (a).

crystals are shown in Fig. 2 as a function of temperature, up to 300 K. The arrows denote the PI to FM transition temperature. For comparison, the temperature variation of the end member polycrystalline sample $Sr_3Mn_2O_7$ ($x=1$) is also presented in Fig. 2(a). We note, first that a low thermal conductivity was observed over a wide range of temperatures for all samples ,in spite of the high quality of our single crystals. Second, the temperature dependence of κ in the ab plane exhibited anomalies associated with the PI to FM transition, while no such anomalies were observed for κ along the c-axis direction near T_C for any of the samples. Above T_C, the value of κ_{ab} showed a positive curvature but tended towards a constant value near room temperatures with increasing temperatures. The electron thermal conductivity for the $z=0$ sample is estimated to be atmost $\sim 1\%$ of the total value, even in the metallic state from the resistivity data based on the Wiedemann-Franz (WF) law and reproduce neither the whole anomaly in κ_{ab} nor the giant thermal effect around T_C.[10] Thus, heat carriers are taken as phonons for all measured samples. Here, the phonon mean free path l_{ph} in the insulating state of the $x=0.4$ sample is estimated from the specific-heat data C_{ph}, and longitudinal sound velocity v_{ph} using the kinetic expression for the phonon gas $\kappa = 1/3 C_{ph} v_{ph} l_{ph}$. If $C_{ph}(150\ \mathrm{K}) = 1.78\ \mathrm{J/cm^3\ K}$ (Ref. 19) and $\kappa_{ab}(150\ \mathrm{K}) = 11.3\ \mathrm{mW/cm}$ (present data) for the $(La_{1-z}Pr_z)_{1.2}Sr_{1.8}Mn_2O_7$ single crystal ($z=0.4$) and $v_{ph} = 4.3\times 10^5$ cm/s (Ref. 20) in the ab plane for the $La_{1.2}Sr_{1.8}Mn_2O_7$ bilayer single crystal, we then obtain $l_{ph,ab} = 4.43$ Å at 150 K, which is comparable with the Mn-O-Mn bond length (~ 4 Å). In a smilar way, the value of $l_{ph,ab}$ reaches 4.07 Åat 300 K. In our estimation, the value of v_{ab} is taken as a constant since the relative variation of the longitudinal velocity is very small from ultrasonic measurements on the bilayer manganites.

Next, the end member compound $Sr_3Mn_2O_7$ showed a different behavior from the ab-plane data in the compound $(La_{1-z}Pr_z)_{1.2}Sr_{1.8}Mn_2O_7$. The value of κ of the $x=1$ sample remained almost a constant down to ~ 200 K, then showed a slight increase upon crossing $T_N = \sim 160$ K and finally dropped rapidly with decreasing temperature. The temperature dependence of κ of the $x=1$ sample reminds us of a typical phonon conduction in insulating materials, except for the magnitude of measured values. The extremely high resistivity of the $x=1$ ($n=2$) sample ($\sim 100\Omega$ cm at RT) in sharp contrast with the value of ρ_{ab} ($\sim 0.1\Omega$ cm at RT) for the Pr-substituted $x=0.4(n=2)$ samples gives rise to a negligible contribution of small polarons, which probably results in a typical phonon conduction. In comparison with the thermal data of the polycrystalline sample of $Sr_3Mn_2O_7$, low thermal values of single-crystal samples are anomalous indicating a strong phonon damping, which correlates with dynamical lattice distortions coupled to thermally hopping of localized carriers at Mn sites (as discussed later).

We discuss the relationship between local lattice distortions and thermal conductivity in bilayer manganites. Figures 3(a) and 3(b) show the anisotropic lattice striction and volume striction for the $z=0$, 0.2, and 0.4 samples, respectively. The anomaly in anisotropic lattice striction reverses sign near $z=0.2$ but the volume of all samples rapidly shrinks upon crossing T_C. These findings have been discussed in Ref. 21 on the basis of different relaxation models of local lattice distortions in metal and insulating states proposed by Medarde *et al.*[15] The authors tried to explain the different behaviors of average and local lattice distortions observed in neutron powder-diffraction experiments on $La_{2-2x}Sr_{1+2x}Mn_2O_7$ ($0.32 \leqslant x \leqslant 0.4$). Based on their expla-

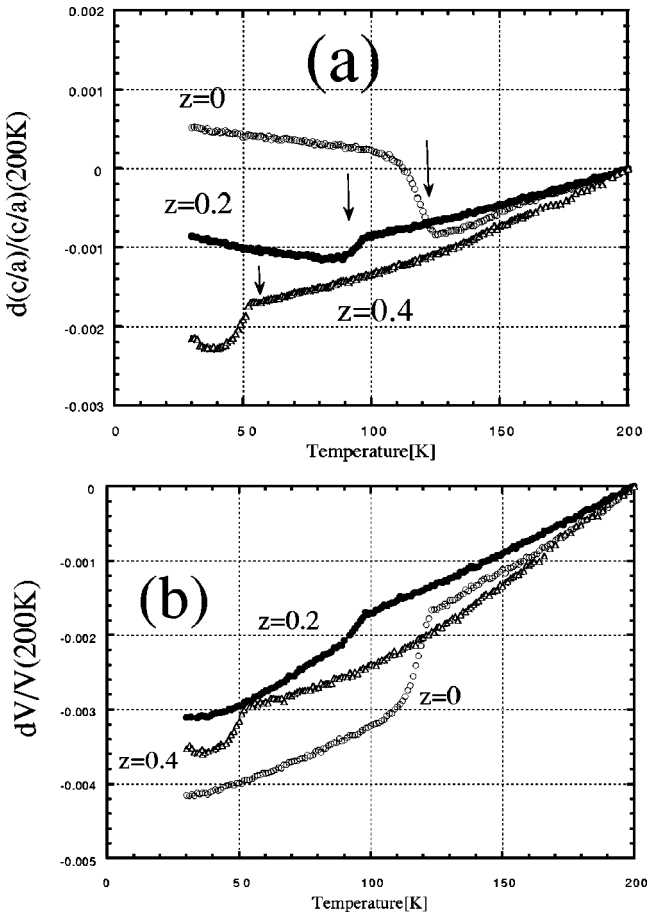

FIG. 3. (a) Anisotropic lattice striction and (b)volume striction, as a function of temperature, up to 300 K, for $(La_{1-z}Pr_z)_{1.2}Sr_{1.8}Mn_2O_7$ ($z=0$, 0.2, 0.4, and 0.6) single crystals. The arrows denote the PI to FM transition temperature.

nation, the observed volume shrinkage near T_C seems to arise from a strong suppression in the local lattice disorder manifested by Mn^{3+}-O_6 and Mn^{4+}-O_6 octahedra with the JT distorted and undistorted sites when the system is going towards the metallic state from the insulating state. The Mn-O bond-length distribution becomes narrower below T_C because of a screening effect due to itinerant carriers. Accordingly, the phonon conduction is limited by the local lattice disorder accompanying a polaron hopping in the insulating state. However, in the metallic region, it is expected that the homogenous structure of the local lattice associated with carrier delocalization causes an upturn in the ab-plane thermal conductivity below T_C. It should be noted that this conclusion is reached from the lattice striction and thermal data of the same samples, combined with the preceding model. Furthermore, in comparison with the anisotropic Debye-Waller (DW) factor of $Sr_3Mn_2O_7$, the anisotropic DW data of $La_{2-2x}Sr_{1+2x}Mn_2O_7$ ($0.32 \leqslant x \leqslant 0.4$) show that even in the metallic state of the latter, the inhomogeneities in the local lattice structure still remain. This finding is probably related not only with a small upturn in κ, but also to the low values of κ. On the other hand, the out-of-plane phonon conduction across the MnO double layers is strongly disturbed from stacking faultlike scattering of the layered structures. Phonon

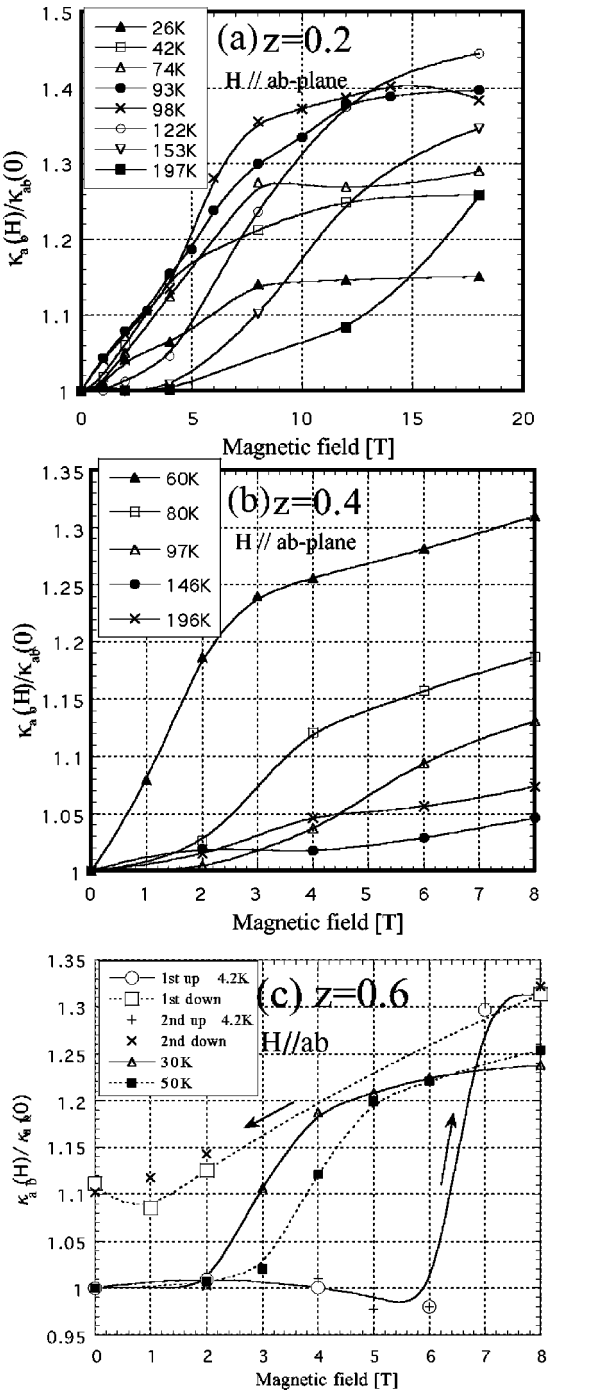

FIG. 4. Normalized magnetothermal conductivity (NMTC) $[\kappa_{ab}(H)/\kappa_{ab}(0)]$ of $(La_{1-z}Pr_z)_{1.2}Sr_{1.8}Mn_2O_7$ ($z=0$, 0.2, 0.4, and 0.6) single crystals. (a)$z=0.2$, (b) $z=0.4$, and (c) $z=0.6$. The field was applied in the ab plane, parallel to the direction of the heat current.

scattering due to stacking faults dominates thermal conduction along the c axis, masks some contribution of the local lattice distortion associated with the insulator to metal transition and results in to the anisotropy of the thermal conductivity.

We discuss next the normalized magnetothermal conductivity (NMTC) $[\kappa_{ab}(H)/\kappa_{ab}(0)]$ of the Pr-substituted crys-

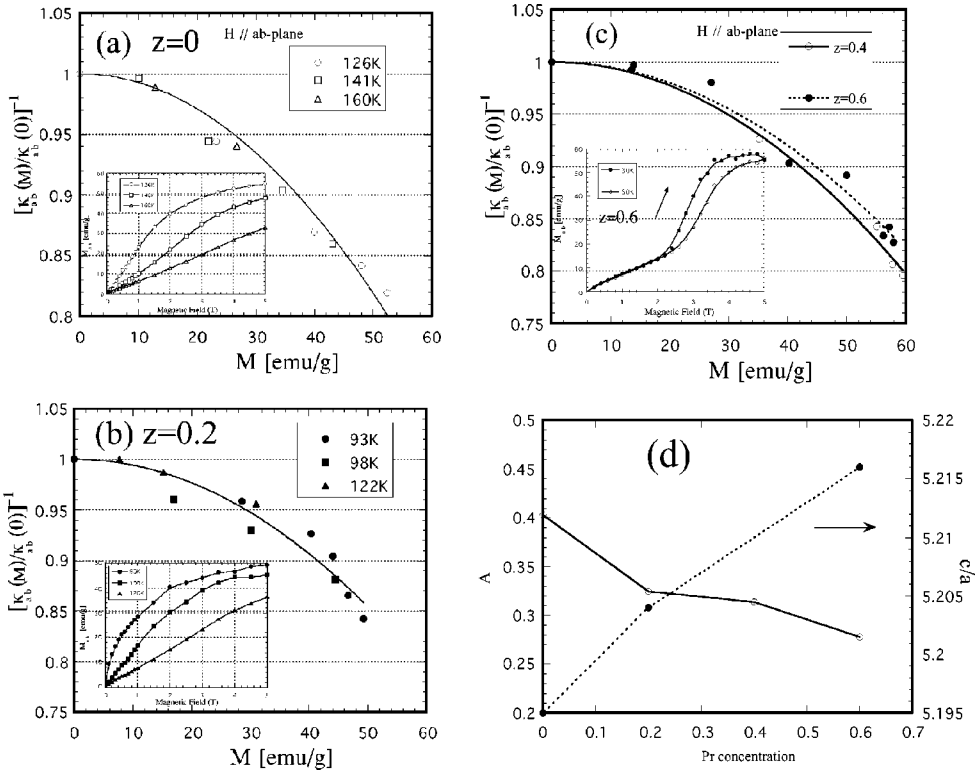

FIG. 5. Normalized magnetothermal resistivity $[\kappa_{ab}(M)/\kappa_{ab}(0)]^{-1}$ of $(La_{1-z}Pr_z)_{1.2}Sr_{1.8}Mn_2O_7$ ($z=0$, 0.2, 0.4, and 0.6) single crystals as a function of magnetization, at selected temperature. (a)$z=0$, (b) $z=0.2$, and (c) $z=0.4$ and 0.6. The insets in (a–c)represent M_{ab}-H curves at the corresponding temperatures for the samples with $z=0$, 0.2, and 0.6, respectively. (d)z dependence of coefficient A and lattice parameter c/a

tals at $z=0.2$, $z=0.4$, and $z=0.6$ (Fig. 4). The field was in the ab plane and parallel to the direction of the heat current. Our data reveal several interesting features. First, a giant magnetothermal conductivity was observed in association with the occurrence of the CMR effect and the NMTC reached about 30%, up to 8 T, for all samples in spite of a lower T_C. Here, it should be noted that $\kappa_c(H)/\kappa_c(0)$ is almost negligible in contrast with a rapid enhancement of $\kappa_{ab}(H)/\kappa_{ab}(0)$, which is consistent with the absence of anomalies observed in $\kappa_c(T)$.[10] Second, accompanying the field-induced first-order PI to FM transition of the insulating sample, $z=0.6$, a clear hysteresis in the magnetothermal conductivity was observed. The remnant NMTC at 4.2 K reached nearly the same value of $\sim 10\%$, both in first and second scans, where after the first scan, the sample was warmed up to high temperatures in order to demagnetize it. The value of NMTC of the $z=0.6$ sample exhibited a steplike behavior at 4.2 K, while it showed a smooth rise with increasing temperature. As previously pointed out, electronic contribution from the WF law estimation using the CMR data reproduces neither an upturn in κ_{ab} nor a giant thermal effect. Magnetostriction data around T_C showed a volume shrinkage upon application of a magnetic field, up to 8 T, as well as a spontaneous striction ($\sim 0.1\%$) upon crossing T_C.[21,22] The negative magnetovolume effect indicates a suppression in local lattice disorder; the reduction in phonon scattering due to structural disorder leads to a giant magnetothermal effect in the same way as the upturn in κ below T_C.

The normalized magnetothermal resistivity $[\kappa_{ab}(M)/\kappa_{ab}(0)]^{-1}$ of our samples is plotted as a function of magnetization at selected temperatures in Figs. 5(a–c), where the insets in Figs. 5(a–c) represent M_{ab}-H curves at the corresponding temperatures for the samples with $z=0$, 0.2, and 0.6, respectively. It is easily found that the value of the magnetothermal resistivity is scaled with a parabolic function of $1-A(M/M_s)$,[2] as pointed out for cubic manganites, by Cohn *et al.*[6] Here, M_s is taken as the value of $3.6\mu_B$ per Mn sites. The coefficient A depends on the value of z and shows a monotonical decrease from 0.4 for $z=0$ down to 0.28 for $z=0.6$, as shown in Fig. 5(d). This finding suggests a suppression of the lattice-spin coupling in thermal CMR due to Pr substitution and can be explained as follows. The Pr substitution had a strong effect on the magnetic anisotropies. The low-temperature magnetic anisotropy M_{ab}/M_c in a field of 100 mT reduced from ~ 10 at $z=0$ to nearly 1 at $z=0.2$ and 0.4. For $z=0.6$, the easy axis of magnetization was along the c axis. On the other hand, the lattice parameters vary with Pr substitution in such a manner that the c axis expands but the $a(b)$ axis shrinks [see Fig. 5(d)], which results in a change of e_g-electron character from planar $3d_{x^2-y^2}$ to linear $3d_{3z^2-r^2}$. Accordingly, such a variation of the e_g-electron character accompanies that of magnetic anisotropy, so that Pr substitution probably suppresses indi-

rectly the lattice-spin coupling in thermal CMR through a variation of spin alignment, strongly coupled with orbital states. In other words, a higher magnetothermal conduction favors the occurrence of the easy axis of magnetization lying in the ab plane. It is an interesting feature that a change of e_g-electron character due to Pr substitution appears in giant magnetothermal effect involving heat carrying phonons.

Finally, we shall stress that at lower temperatures, far from T_C, a finite increase of κ_{ab} ($\sim$14% at 8 T) for the $z=0.2$ crystal was observed. If we accept the above explanation, this finding indicates that phonon scattering due to local lattice disorder (bond-length fluctuation) remains, even in the metallic state, which is consistent with the anisotropic DW data of $La_{2-2x}Sr_{1+2x}Mn_2O_7$ ($0.32 \leqslant x \leqslant 0.4$) in the metallic state. Recently, Maezono and Nagaosa[23] pointed out that in manganite systems, the dynamic JT effect is more enhanced in the metallic region than in the insulating region because of strong electron correlations. Magnetothermal measurements at low temperatures probe the lattice disorder not only in the insulating region but also in the metallic region as the DW factor does. Furthermore, it is desirable to clarify the crucial role played by the dynamic local lattice distortion on phonon conduction not only in the insulating phase, but also in the metallic phase through magnetothermal measurements on high-quality single crystal of the highly doped bilayer compounds.

In summary, a systematic study of thermal conductivity as a function of temperature and magnetic field of single crystals of the compound $(La_{1-z}Pr_z)_{1.2}Sr_{1.8}Mn_2O_7$ for $z(Pr)=0.2$, 0.4, and 0.6 was performed. The ab-plane phonon conduction of the Pr-substituted $x=0.4$ samples is disturbed by the dynamical lattice distortions associated with polaron hopping on Mn sites. On the other hand, the typical phonon behavior observed for the end member $x=1$ sample is probably attributed to a reduction of the inhomogeneities in the local lattice distortions strongly coupled with small polarons. The giant magnetothermal effect has been explained taking into account a systematic variation of the e_g-electron orbital states due to Pr substitution.

ACKNOWLEDGMENTS

The authors would like to thank Dr. H. Ogasawara for his technical support. This work was supported by a Grant-in-Aid for Scientific Research from the Ministry of Education, Science, and Culture, Japan.

[1] *Colossal Magnetoresistance, Charge Ordering and Related Properties of Manganese Oxides*, (edited by C.N.R. Rao and B. Raveau (World Scientific, Singapore, 1988); *Colossal Magnetoresistive Oxides*, edited by Y. Tokura (Gordon and Breach, New York, 2000).

[2] C. Zener, Phys. Rev. **82**, 403 (1951); P.G. de Gennes, *ibid.* **118**, 141 (1960).

[3] A.J. Millis, P.B. Littlewood, and B.I. Shraiman, Phys. Rev. Lett. **74**, 5144 (1995); A.J. Millis, B.I. Shraiman, and R. Mueller, *ibid.* **77**, 175 (1996).

[4] For a recent review, see E. Dagotto, T. Hotta, and A. Moreo, Phys. Rep. **344**, 1 (2001).

[5] D.W. Visser, A.P. Ramirez, and M.A. Subramanian, Phys. Rev. Lett. **78**, 3947 (1997).

[6] J.L. Cohn, J.J. Neumeier, C.P. Popoviciu, K.J. McClellan, and Th. Leventouri, Phys. Rev. B **56**, R8495 (1997).

[7] S. Uhlenbruck, B. Buchner, R. Gross, A. Freimuth, A. Maria de Leon Guevara, and A. Revcolevschi, Phys. Rev. B **57**, R5571 (1998).

[8] J. Hejtmanek, Z. Jirak, M. Marysko, S. Krupicka, C. Martin, A. Maignan, M. Hervieu, and B. Raveau, Phys. Rev. B **60**, 14 057 (1999).

[9] Y. Moritomo, A. Asamitsu, H. Kuwahara, and Y. Tokura, Nature (London) **380**, 141 (1996).

[10] M. Matsukawa, H. Ogasawara, R. Sato, M. Yoshizawa, R. Suryanarayanan, G. Dhalenne, A. Revcolevschi, and K. Itoh, Phys. Rev. B **62**, 5327 (2000).

[11] J.S. Zhou and J.B. Goodenough, Phys. Rev. B **64**, 024421 (2001).

[12] H. Ogasawara, M. Matsukawa, S. Hatakeyama, M. Yoshizawa, M. Apostu, R. Suryanarayanan, G. Dhalenne, A. Revcolevschi, K. Itoh, and N. Kobayashi, J. Phys. Soc. Jpn. **69**, 1274 (2000).

[13] M. Apostu, R. Suryanarayanan, A. Revcolevschi, H. Ogasawara, M. Matsukawa, M. Yoshizawa, and N. Kobayashi, Phys. Rev. B **64**, 012407 (2001).

[14] Y. Moritomo, Y. Maruyama, T. Akimoto, and A. Nakamura, Phys. Rev. B **56**, R7057 (1997).

[15] M. Medarde, J.F. Mitchell, J.E. Millburn, S. Short, and J.D. Jorgensen Phys. Rev. Lett. **83**, 1223 (1999).

[16] N. Mizutani, A. Kitazawa, O. Nobuyuki, and M. Kato, J. Chem. Soc. (Japan) Ind. Ed. **73**, 1097 (1970).

[17] J.F. Mitchell, J.E. Millburn, M. Medarde, D.N. Argyriou, and J.D. Jorgensen, J. Appl. Phys. **85**, 4352 (1999).

[18] H. Meskine, Z.S. Popovic, and S. Satpathy, Phys. Rev. B **65**, 094402 (2002).

[19] A. Vasilev, T. Voloshok, M. Apostu, R. Suryanarayanan, A. Revcolevschi, JETP Lett. **73**, 630 (2001).

[20] C.N. Brosseau, M. Poirier, R. Suryanarayanan, G. Dhalenne, and A. Revcolevschi, cond-mat/0012380 (unpublished).

[21] M. Matsukawa, H. Ogasawara, T. Sasaki, M. Yoshizawa, M. Apostu, R. Suryanarayanan, A. Revcolevschi, K. Itoh, and N. Kobayashi, J. Phys. Soc. Jpn. **71**, 1475 (2002).

[22] T. Kimura, Y. Tomioka, A. Asamitsu, and Y. Tokura, Phys. Rev. Lett. **81**, 5920 (1998).

[23] R. Maezono and N. Nagaosa, Phys. Rev. B **67**, 064413 (2003).